12-1-2016

Atp2c2 Is Transcribed From a Unique Transcriptional Start Site in Mouse Pancreatic Acinar Cells

Melissa A. Fenech
Children's Health Research Institute, London, ON

Caitlin M. Sullivan
Children's Health Research Institute, London, ON

Lucimar T. Ferreira
Children's Health Research Institute, London, ON

Rashid Mehmood
Children's Health Research Institute, London, ON

William A. MacDonald
Magee-Womens Research Institute

See next page for additional authors

Journal of Cellular Physiology

Atp2c2 Is Transcribed From a Unique Transcriptional Start Site in Mouse Pancreatic Acinar Cells

MELISSA A. FENECH,[1,2,3] CAITLIN M. SULLIVAN,[1,2,3] LUCIMAR T. FERREIRA,[1,2] RASHID MEHMOOD,[1,2] WILLIAM A. MACDONALD,[4] PETER B. STATHOPULOS,[3] AND CHRISTOPHER L. PIN[1,2,3,5]*

[1]*Children's Health Research Institute, London, Ontario, Canada*

[2]*Department of Pediatrics, University of Western Ontario, London, Ontario, Canada*

[3]*Department of Physiology and Pharmacology, University of Western Ontario, London, Ontario, Canada*

[4]*Magee-Womens Research Institute and Department of Obstetrics, Gynecology and Reproductive Sciences, University of Pittsburgh School of Medicine, Pittsburgh, Pennsylvania*

[5]*Department of Oncology, University of Western Ontario, London, Ontario, Canada*

Proper regulation of cytosolic Ca^{2+} is critical for pancreatic acinar cell function. Disruptions in normal Ca^{2+} concentrations affect numerous cellular functions and are associated with pancreatitis. Membrane pumps and channels regulate cytosolic Ca^{2+} homeostasis by promoting rapid Ca^{2+} movement. Determining how expression of Ca^{2+} modulators is regulated and the cellular alterations that occur upon changes in expression can provide insight into initiating events of pancreatitis. The goal of this study was to delineate the gene structure and regulation of a novel pancreas-specific isoform for Secretory Pathway Ca^{2+} ATPase 2 (termed SPCA2C), which is encoded from the *Atp2c2* gene. Using Next Generation Sequencing of RNA (RNA-seq), chromatin immunoprecipitation for epigenetic modifications and promoter-reporter assays, a novel transcriptional start site was identified that promotes expression of a transcript containing the last four exons of the *Atp2c2* gene (*Atp2c2c*). This region was enriched for epigenetic marks and pancreatic transcription factors that promote gene activation. Promoter activity for regions upstream of the ATG codon in *Atp2c2*'s 24th exon was observed in vitro but not in in vivo. Translation from this ATG encodes a protein aligned with the carboxy terminal of SPCA2. Functional analysis in HEK 293A cells indicates a unique role for SPCA2C in increasing cytosolic Ca^{2+}. RNA analysis indicates that the decreased *Atp2c2c* expression observed early in experimental pancreatitis reflects a global molecular response of acinar cells to reduce cytosolic Ca^{2+} levels. Combined, these results suggest SPCA2C affects Ca^{2+} homeostasis in pancreatic acinar cells in a unique fashion relative to other Ca^{2+} ATPases.

J. Cell. Physiol. 231: 2768–2778, 2016.

Pancreatic acinar cells are polarized with highly organized intracellular compartments that permit rapid receptor-regulated exocytosis of enzymes. The precise spatial and temporal control of Ca^{2+} release is fundamental for proper exocytosis of enzymes (Lee et al., 1997). The ability for Ca^{2+} to act as a second messenger in enzyme release is provided by the maintenance of a cytosolic Ca^{2+} gradient with greater concentrations of Ca^{2+} outside the cell or within intracellular compartments such as the ER, relative to the cytosol. Transient increases in cytosolic Ca^{2+} are coupled to exocytosis of zymogen granules (ZG) containing enzymes (Burnham and Williams, 1984), while dysregulation of intracellular Ca^{2+} concentration affects gene transcription, cell proliferation, apoptosis, or necrosis and is associated with the initiation of pancreatitis (Zhou et al., 1996; Kruger et al., 2000; Li et al., 2014).

The ability to restore the cytosolic Ca^{2+} gradient after ER release is due, in part, to P-type Ca^{2+} ATPases that remove Ca^{2+} from the cytosol (Lee et al., 1997). There are three families of P-type Ca^{2+} ATPases. Sarcoendoplasmic reticulum Ca^{2+}ATPases (SERCAs; encoded by three *Atp2a* genes) translocate Ca^{2+} into the ER (Zhao et al., 2001; Arredouani et al., 2002; Beauvois et al., 2004). Plasma membrane Ca^{2+} ATPases (PMCAs; encoded by four *Atp2b* genes) translocate Ca^{2+} out of the cell. The third type of Ca^{2+} ATPase is the secretory pathway Ca^{2+} ATPases (SPCAs, encoded by two *Atp2c* genes), which translocate Ca^{2+} into the Golgi (reviewed in Vanoevelen et al., 2007; He and Hu, 2012). SPCA1/*Atp2c1* is a homolog of Pmr1/*PMR1* first described in *Saccharomyces cervisiae* (Rudolph et al., 1989). SPCA1 is ubiquitously expressed and targeted deletion of *Atp2c1* in mice results in gestational growth retardation and death before embryonic day 10.5 (Okunade et al., 2007). In humans, mutations in the *ATP2C1* are found in Hailey–Hailey disease (Sudbrak et al., 2000). A second isoform, SPCA2/*Atp2c2* is expressed only in higher organisms (mammals) and is limited to a few tissues, including secretory and absorptive epithelia of the gastrointestinal, genitourinary, mammary, and salivary glands (Vanoevelen et al., 2005). Unlike SPCA1, SPCA2 appears to

Melissa Fenech and Caitlin M. Sullivan contributed equally to the work.

Conflicts of interest: none.

Contract grant sponsor: Natural Sciences and Engineering Research Council;
Contract grant number: 250225.
Contract grant sponsor: Children's Health Foundation.

*Correspondence to: Christopher Pin, Department of Pediatrics, University of Western Ontario, Children's Health Research Institute, 5th Floor, Victoria Research Laboratories, London, Ontario N6C 2V5, Canada. E-mail: cpin@uwo.ca

Manuscript Received: 28 December 2015
Manuscript Accepted: 24 March 2016

Accepted manuscript online in Wiley Online Library (wileyonlinelibrary.com): 27 March 2016.
DOI: 10.1002/jcp.25391

have a broader localization pattern in the cell, found in the Golgi, ER, and secretory vesicles (Xiang et al., 2005; Feng et al., 2010; Garside et al., 2010; Pestov et al., 2012).

SPCA2 is found only in higher functioning organisms; however, its definitive function is yet to be determined. In lactating gland luminal epithelial, SPCA2 is localized predominantly to vesicles that travel to the plasma membrane rather than the Golgi and has a major role in increasing intracellular Ca^{2+} (Cross et al., 2013). Human breast adenocarcinoma MCF7 cells have higher SPCA2 expression compared to MCF-10A, a non-malignant human mammary epithelial cell line. Increased SPCA2 expression was also observed in a small group of breast cancer patients suggesting a potential link between SPCA2, cytosolic Ca^{2+}, and metastasis (Feng et al., 2010). These studies also suggest that truncations of SPCA2 may be involved in Store Independent Ca^{2+} Entry (SICE) by activating ORAI1 protein function (Feng and Rao, 2013).

SPCA2 is translated from the *Atp2c2* gene that spans a region of 95.5 kb on human chromosome 16, which contains 27 exons. SPCA2 is 946 amino acids long (Vanoevelen et al., 2005). SPCA2 is expressed in pancreatic acinar cells, but characterization of SPCA2 expression indicated a significantly smaller protein (Garside et al., 2010) than the predicted full length SPCA2 (Vanoevelen et al., 2005; Pestov et al., 2012). Expression analysis of this smaller SPCA2 isoform suggested a novel function from the full length SPCA2 as it was localized to both the Golgi and ER. Relevant to acinar cell physiology, SPCA2 expression was markedly decreased in *Mist1*$^{-/-}$ mice, which show defects in Ca^{2+} handling (Garside et al., 2010). This study also suggests that MIST1 may directly regulate pancreatic expression of *Atp2c2*. While it is clear that the pancreatic isoform, termed SPCA2C, contains at least the carboxy terminus of SPCA2, without knowledge of the exact transcriptional start site and exon/intron structure; it is unclear what functional significance SPCA2C has in Ca^{2+} homeostasis. To appropriately study the function and regulation of SPCA2/*Atp2c2* in the pancreas, it is imperative to determine if *Atp2c2c* is the result of altered splicing or a pancreatic-specific transcriptional start site (TSS).

The goals of this study were to determine the complete *Atp2c2* transcript encoding SPCA2C, delineate factors regulating *Atp2c2* expression in the pancreas, and determine if SPCA2C affects Ca^{2+} homeostasis. Our results show that *Atp2c2* is transcribed from a unique TSS in pancreatic acinar tissue, encoding only the carboxy terminal portion of SPCA2. In addition, over expressing SPCA2C is accompanied by persistent elevation in cytosolic Ca^{2+}, revealing a novel role for SPCA2C in regulating acinar cell function.

Materials and Methods

Mouse handling and initiation of cerulein-induced pancreatitis

C57Bl/6 mice were used for all experiments except for transgene analysis. Mice were handled according to guidelines approved by the Animal Care and Use Subcommittee at the University of Western Ontario (Protocols 2008-116 and 2008-027). Transgenic mice carrying the *−1181 + 57Atp2c2* promoter region upstream of a *LacZ* reporter gene were generated through pronuclear injection of CBA/C57BL/6 hybrid zygotes followed by implantation into CD1 pseudopregnant mice. Founder mice (F0) were mated to C57Bl/6 mice, and 3–4-week-old F1 mice characterized for transgene expression. 2–4-month-old male C57Bl/6 animals were used for gene, ChIP, and RNA-seq analysis. The targeted deletion of the *Mist1* gene has previously been described (Pin et al., 2001). Cerulein-induced pancreatitis (CIP) was initiated as described (Kowalik et al., 2007) with 4–8 hourly intraperitoneal injections of 50 μg/kg cerulein (cholecystokinin analog) and mice sacrificed 4, 8, 32, and 72 h after initial injection.

RNA isolation, qRT-PCR, and RNA-Seq

RNA was isolated from mouse pancreatic tissue using 5′ Prime isol-RNA Lysis Reagent (Fisher Scientific, Burlington, ON) followed by PureLink RNA Mini Kit (Life Technologies, Waltham, MA). RNA-seq was performed by The Centre for Applied Genomics at The Hospital for Sick Children (Toronto, ON). The full details of the RNA-seq will be provided elsewhere (Fazio et al., unpublished; GEO accession number to follow).

ChIP-PCR, chIP-seq, and bioinformatics analysis

Chromatin was isolated from pancreatic tissue of C57/Bl6 mice or *Mist1*$^{-/-}$ pancreatic tissue mice as described (Johnson et al., 2014; Mehmood et al., 2014). Chromatin immunoprecipitation (ChIP) was performed using antibodies specific for MIST1 (Johnson et al., 2004), Histone 3 lysine 36 trimethylation (H3K36Me3; Abcam, Cambridge, MA), RNA polymerase II (Millipore, Temecula, CA), H3K4Me3, and H3K27Me3 as described (Mehmood et al., 2014). ChIP was followed by qPCR using the GoTaq PCR Mastermix system (Promega, Madison, WI). Samples were evaluated using the ABI Prism 7900HT Sequence Detection System and Vii A7 RUO software (Applied Biosystems, Foster City, CA). Average Ct values for individual ChIP and IgG controls were expressed as a percent of starting chromatin samples (input). Alternatively, H3K4Me3 ChIP was followed by Next Generation sequencing (ChIP-Seq; the complete dataset is described (Mehmood et al., 2014).

Plasmid construction

Putative promoter regions upstream of the ATG codon in exon 24 of the *Atp2c2* gene (Supplementary Fig. S1), which corresponds to +2,580 (RNA sequence) or +54,891 (DNA sequence) in the full length *Atp2c2* sequence were designed based on the UCSC Genome browser identification of *Atp2c2* (uc009nqg.1) and constructed by Invitrogen GeneArt (Regensburg, Germany). The *Atp2c2-Luciferase2* sequence was cloned into *pGL3Basic* using *Xho1* and *HindIII* cloning sites and verified by Sanger sequencing. The final promoter-reporter constructs were designated in relationship to the first base pair based on ChIP-seq data and include *−1181 + 57Atp2c2cpGL3*, *−562 + 57Atp2c2cpGL3*, and *−252 + 57Atp2c2cpGL3* (Supplementary Fig. S1). A similar approach was used to generate a 1238 bp region upstream of the ATG codon found in exon 23 (*Alt-ATG-Atp2c2pGL3*). Promoter-less pGL3 and pWHERE plasmids were used as negative controls for all transfection assays.

To generate a transgene promoter construct, *−1181 + 57Atp2c2cpGL3* was digested with *XhoI* and *SmaI* and cloned into *pWHERE* (Invitrogen, San Diego, CA) digested with the same enzymes. Finally, a *pcDNA3.1* expression vector containing the exact SPCA2C reading frame was generated by GeneArt using sequence information from NCBI (Accession #AC_000030.1). The *Atp2c2c* sequence was followed by the FLAG antigenic tag sequence (5′ GATTACAAGGATGACGACGATAAG 3′; *pcDNA-SPCA2*^{FLAG}) and then a stop codon.

Cell culture and luciferase assays

Human embryonic kidney (HEK) 293A cells were maintained in Dulbecco's Modified Eagle Medium (DMEM) high glucose media (HyClone, Logan, UT) containing 10% FBS and 1% Penstrep. When cultures reached 70–80% confluence, cells were transfected using JetPrime transfection kit, with *Atp2c2c* promoter-luciferase or promoter-*LacZ* plasmids described above. Promoter-less *pGL3* and *pWHERE* plasmids were used as controls. Forty-eight hours after transfection, protein was isolated using the Dual-Luciferase Reporter Assay Kit (Promega). Luciferase analysis was performed in triplicate using the Lumat LB 9507 Luminometer (Berthold

Technologies, Oakridge, TN). Firefly *luciferase* amounts were normalized to *Renilla luciferase* values, and this ratio normalized to expression of *pGL3-Basic*. Data was analyzed using GraphPad Prism software version 6.0 by two way analysis of variance (ANOVA) with a Bonferroni post hoc test. Graphs show mean values ± standard error of measure (SEM).

Calcium imaging

HEK293 cells were transfected as described above with *pcDNA3.0GFP*, *pcDNA3.1-SPCA2C*^{FLAG}, or *pcDNA3.1-SPCA2*^{MYC} (encodes full length SPCA2; kindly provided by R. Rao; (Feng et al., 2010). Forty-eight hours after transfection cells were loaded with Fura-2 AM at 1 μM in culture media (Dulbecco's Modified Eagle Medium (DMEM) high glucose media (HyClone) containing 10% FBS and 1% Penstrep) for 30 min at 37°C and 5% CO_2. After loading, cells were rinsed once in Hank's Buffered Saline Solution (HBSS; 140 mM NaCl, 4.7 mM KCl, 1.13 mM MgCl, 10 mM glucose, 10 mM HEPES, 1.8 mM CaCl) and then allowed to rest for 10 min at room temperature in HBSS before recording started. Cells were excited at 340 nm and 380 nm, and Fura2 emissions at 505 nm were measured per individual cell. Changes in the Fura-2 fluorescence ratio using excitation wavelengths of 340/380 nm were taken as a measure of changes in intracellular Ca^{2+} levels while individual groups of cells were stimulated with 10 μM carbachol for 5 min at a pressure of 2 Pa by puffing. Five-minute puffing experiments were completed no more then three times per plate, and never on the same group of cells. N values are provided for each study within the figure legends. Data is shown +/− SEM and significance was determined using a one way ANOVA and Tukey's posthoc test.

Immunofluorescence analysis

HEK293 cells were transfected as described above with *pcDNA3.1-SPCA2C*^{FLAG} and/or *pcDNA3.1-SPCA2*^{MYC}. Forty-eight hours after transfection, HEK293 cells were fixed with 4% formaldehyde in PBS. IF was performed as described (Garside et al., 2010). A mouse antibody for FLAG (diluted 1:500, Sigma) or rabbit antibody specific for MYC (1:1000, Sigma), were diluted in blocking solution (PBS, 5% BSA, 1% triton). Fluorescently labelled secondary goat antibodies were diluted 1:250 in PBS (Jackson Immunoresearch Labs, West Grove, PA or Sigma, Oakville, ON, Canada). We acquired confocal images using a Leica SP5 Confocal microscope and the colocalization finder plugin for ImageJ (http://1.usa.gov/1Pn0ru1) was used to determine overlap of fluorochromes.

Results

The pancreatic isoform of *Atp2c2*/SPCA2 is significantly smaller (Garside et al., 2010) than the published full-length molecule that has been reported in the literature (Vanoevelen et al., 2005). However, it is unclear whether the pancreas transcript (termed *Atp2c2c*; c for carboxy) was the result of an alternative transcriptional start site (TSS) or alternative splicing of the larger *Atp2c2* transcript. To resolve this question, the *Atp2c2* genomic region was visualized with the USCS Genome browser using RNA-seq data on total pancreatic tissue from 2-month-old mice (Fig. 1A). Examination of the complete *Atp2c2* gene showed no sequence enrichment in exons 1–23, indicating that these exons were not transcribed within the pancreatic genome. Sequence alignment was observed ~41 bp into exon 24 (Fig. 1B), corresponding to +2403 in the full-length transcript, and included all of the remaining exons (24–27) of the *Atp2c2* gene (Supplemental Fig. S3). Examination of other *Atp2* genes showed no unique splicing variants but a potential alternative TSS for *Atp2b1* (Supplementary Fig. S2A). Examination of RNA-seq data from other regions of the gastrointestinal tract (GEO accession number: GSE36025) showed some enrichment along the entire *Atp2c2* gene with greater sequence enrichment of exons near the 3′ end of the *Atp2c2* gene (Supplementary Fig. S4), suggesting that other tissues may contain unique isoforms for *Atp2c2* as well as heterogeneity in the *Atp2c2* isoform expressed. However, none of these tissues express only the pancreatic isoform we have identified.

Several Expressed Sequence Tags (ESTs) have been identified for *Atp2c2*, but only EST AK00749.1, previously identified in a 10-day-old pancreatic EST library, showed alignment to *Atp2c2c* (Fig. 1A and B). Interestingly, alignment of the AK00749.1 sequence with the full length *Atp2c2* identifies a single missing G nucleotide, which is not missing in our RNA-seq data, indicating that *Atp2c2c* perfectly aligns with the last 702 bp of *Atp2c2*.

Based on the RNA-seq and AK00749.1 sequences, we designated the first bp of the *Atp2c2c* transcript as +41 bp into exon 24 of the *Atp2c2* gene. Examination of the *Atp2c2c* sequence identified an open reading frame that initiates from an ATG codon at +57 into *Atp2c2c* and produces a protein that perfectly aligns with the last 136 amino acids of SPCA2 (designated SPCA2C; Fig. 2A; Supplementary Fig. S3). SPCA2C contains the last four transmembrane domains, part of the cation ATPase domain and a cation binding site found within SPCA2 (Supplementary Fig. S3B).

The region upstream of the *Atp2c2c* TSS was examined for putative transcription factor binding motifs using the Alibaba-Gene Regulation Data Base and Nsite—softberry (http://www.softberry.com). Several binding motifs were identified including NFκB-TNFα-K.3 (NF-κB), Sp1-Ku80 (Sp1), and NF-IL6-CCR1 (NF-IL6) consensus sites (data not shown). However, no consensus TATA box sequence was observed within this region. Therefore, to confirm that the 23rd intron and initial part of the 24th exon of the *Atp2c2* gene drive expression of *Atp2c2c*, we took two approaches. First, this region of *Atp2c2* was characterized for the enrichment of epigenetic marks consistent with TSSs (Fig. 2). Trimethylation of Histone 3 lysine 4 (H3K4Me3) typically occurs at primed or active TSSs (Ruthenburg et al., 2007). Examination of previously published ChIP-seq data for H3K4Me3 enrichment (Mehmood et al., 2014) in pancreatic acinar cells identified significant enrichment at exon 24, but not at any other part of the *Atp2c2* gene, even the TSS for the full length transcript (Fig. 2A). We confirmed specific enrichment for H3K4Me3 at exon 24 using targeted ChIP-qPCR along the *Atp2c2* gene (Fig. 2B and C). Since H3K4Me3 can also mark distal enhancer regions (Pekowska et al., 2011), ChIP-qPCR was performed for epigenetic marks that occur near TSSs, including H3 acetylation (H3Ac), H3K36Me3, and RNApol II. In each case, increased enrichment was observed around exon 24 of the *Atp2c2* gene (Fig. 2D), supporting this region as a novel TSS.

As a second approach to demonstrate promoter activity of this region in the *Atp2c2* gene, regions extending 1238 bp (*−1181 + 57pGL3*), 619 bp (*−562 + 57pGL3*), and 309 bp (*−252 + 57pGL3*) from the starting ATG codon within *Atp2c2* exon 24 were placed in front of a *luciferase* reporter gene (Fig. 3A). As a control, a separate 1238 bp sequence upstream of an ATG codon within exon 23 (*Alt-ATG-Atp2c2pGL3*) was tested. Transient transfection into HEK 293A cells revealed significantly increased activity for *−1181 + 57pGL3*, *−562 + 57pGL3*, and *−252 + 57pGL3* compared to the pGL3 vector alone (Fig. 3B). The *Alt-Atp2c2pGL3* construct showed no such activity (Fig. 3B). Similar promoter activity was observed when the *−1181 + 57* sequence region was placed upstream of a nuclear *LacZ* cassette (*−1181 + 57pWHERE*). Distinct β-galactosidase expression was observed upon transfection in HEK 293A (Fig. 3C) again confirming promoter activity. To determine if the *−1181 + 57pWHERE* promoter-reporter construct was active in vivo, we generated several transgenic lines through pronuclear injection (Fig. 3D). In total,

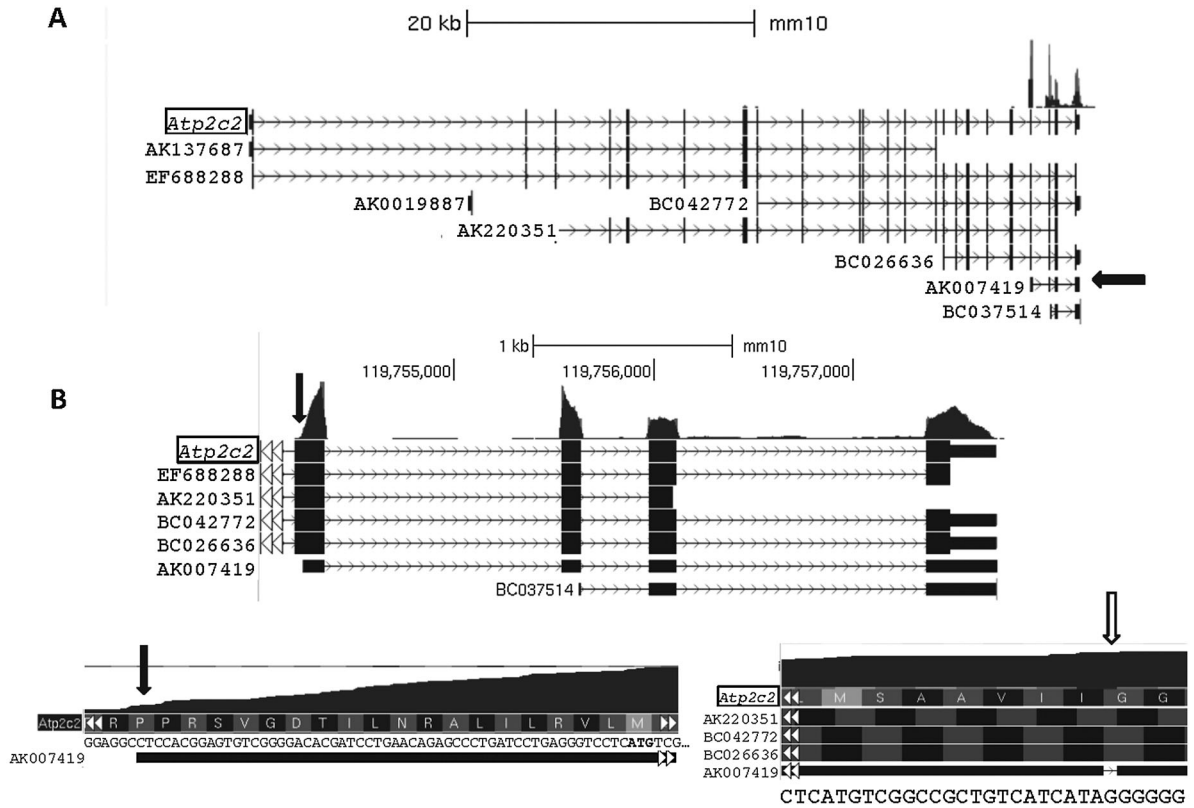

C

```
1     GCTCCACGGAGTGTCGGGGACACGATCCTGAACAGAGCCCTGATCCTGAGGGTCCTCATGTCGGCCGCTGTC
                                                      M  S  A  A  V
73    ATCATAGGGGGGACCCTCTTTATCTTCTGGAGAGAGATCCCAGCGAACGGCACCAGCACCCCACGTACAACC
       I  I  G  G  T  L  F  I  F  W  R  E  I  P  A  N  G  T  S  T  P  R  T  T
145   ACCATGGCCTTCACCTGCTTCGTGTTTTTCGACCTCTTCAATGCCCTGAGCTGTCGCTCTCAGACCAAGCTG
       T  M  A  F  T  C  F  V  F  F  D  L  F  N  A  L  S  C  R  S  Q  T  K  L
217   ATATTTGAGATTGGCTTTTTCCGGAACCGCATGTTCCTGTACTCAGTCCTTGGGTCCCTCCTGGGGCAGCTG
       I  F  E  I  G  F  F  R  N  R  M  F  L  Y  S  V  L  G  S  L  L  G  Q  L
289   GCCGTGATCTATGCCCCGCCCCTACAAAAGGTCTTCCAGACTGAAAACCTGAGCGCGCTCGACCTGCTGCTG
       A  V  I  Y  A  P  P  L  Q  K  V  F  Q  T  E  N  L  S  A  L  D  L  L  L
361   CTGACGGGCCTGGCCTCGTCTGTCTTCATTCTGTCGGAGCTGCTCAAGCTCTGGGAAAAGTTCTTGTCCAGA
       L  T  G  L  A  S  S  V  F  I  L  S  E  L  L  K  L  W  E  K  F  L  S  R
433   GCCAGGCCCACTCAGATGCTCCCGGAAGCTGTGTAACGGAACCAGTGTGTCAAGGCCCTGACTGACCTGTGT
       A  R  P  T  Q  M  L  P  E  A  V  *
505   GCTTGGGTGCCTCTGGCCTGTCCCCATCCATCTGTACTAACCACTCCAAGGGGCAATTCTCAGGACCGTGCA
577   GCATCGGACGCTGGCTCCACCTGTCCTCCTGGCCTGCTGGGCCATGTCCCGCACAGGACAGGGTGGAGCTTA
649   TTATACTGAAACGTGGCGCTATTTATTAAACCACCGTGGTTTTTTTATTTAACTC
```

Fig. 1. Transcription from the *Atp2c2* gene is limited to the last four exons within pancreatic tissue. A: RNA-seq visualization of the *Atp2c2* gene reveals sequence enrichment only with exons 24 to 27. The only EST that corresponds with this sequence is AK007419 (arrow). B: Higher resolution of the RNA-seq data indicates that *Atp2c2c* starts within the 4th exon, exactly where the AK007419 EST begins (downward arrow). However, *Atp2c2c* contains the single G nucleotide missing within the published sequence for AK007419 (open arrow). C: The *Atp2c2c* sequence produces an open reading frame that generates a 136 aa protein that aligns with the carboxy terminus of SPCA2.

nine founder lines were identified containing *−1181 + 57pWHERE*. Evaluation of pancreatic tissue using whole mount β galactosidase analysis revealed no detectable expression above control levels (data not shown). In an attempt to identify more limited expression, we performed RT-PCR analysis for *LacZ* mRNA (Fig. 3E). No detectable *LacZ* expression could be discerned. These findings suggest that the 1181 bp promoter region for *Atp2c2c* does not contain all of the regulatory elements required for pancreatic-specific expression.

Atp2c2c expression is significantly reduced in mice lacking the transcription factor MIST1 (*Mist1*$^{-/-}$; Garside et al., 2010),

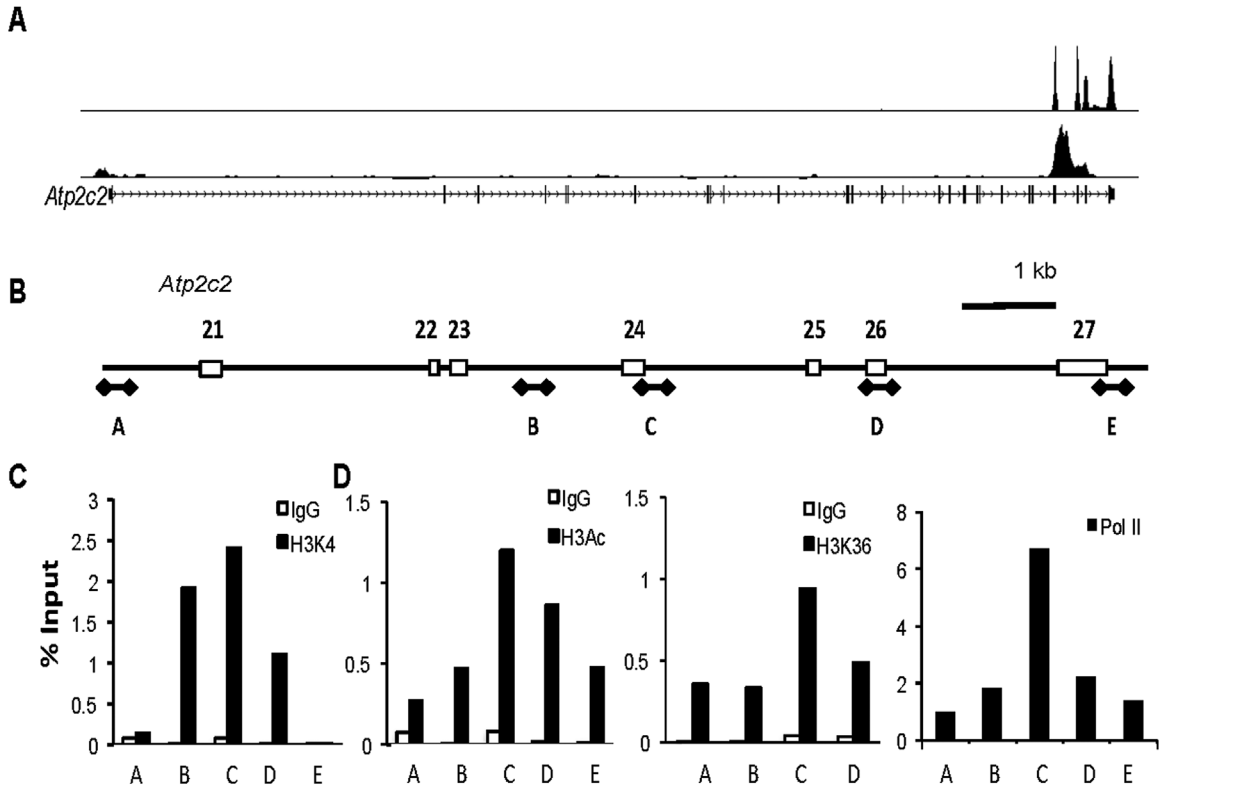

Fig. 2. Enrichment for epigenetic histone modifications and transcription factors are observed at exon 24 within the *Atp2c2* gene. A: Alignment of RNA-Seq of whole pancreatic RNA to the *Atp2c2* gene in wild type (WT) mice was compared to ChIP-seq for H3K4Me3 (K4Me3) enrichment in WT pancreatic tissue. B: Schematic showing the regions of the *Atp2c2* gene amplified by targeted ChIP-qPCR. A–E: represent the putative amplicons generated by ChIP-PCR. ChIP-qPCR for (C) H3K4Me3 or (D) H3 acetylation (H3Ac), H3K36Me3, and RNA polymerase II (PolII) reveals increased enrichment around exon 24. In all cases, n = 3.

which is a model of increased pancreatitis susceptibility with deficits in Ca^{2+} homeostasis (Kowalik et al., 2007). Supporting the existence of the 24th exon of *Atp2c2* containing a TSS, ChIP-seq for H3K4Me3 in pancreatic tissue from *Mist1*$^{-/-}$ mice revealed a marked loss in enrichment, consistent with decreased expression (Fig. 4A). ChIP-PCR and ChIP-qPCR also showed enrichment for MIST1 near the TSS in exon 24 (Fig. 4B and C) suggesting it directly regulates *Atp2c2c* expression.

Based on this decrease in expression in *Mist1*$^{-/-}$ mice, we predicted that *Atp2c2c* expression may also be altered in response to cerulein-induced pancreatitis (CIP). Cerulein is a CCK analogue that at pharmacological levels initiates a pancreatitis response that involves premature enzyme activation, altered cell signalling, and initiation of inflammatory genes (Williams et al., 2002). RNA-seq showed a rapid decrease in *Atp2c2c* expression 4 h after initiating CIP (Fig. 4D and E), which was confirmed by qRT-PCR (Fig. 4F). *Atp2c2c* expression remained low in CIP treated mice relative to saline-treated mice even as long as 72 h after initial injection. Interestingly, *Atp2c2c* expression showed a markedly different response compared to the genes encoding other Ca^{2+} ATPases (Fig. 4G; Supplementary Fig. S2B; and Table 1). All other *Atp2* genes showed either no difference or increased expression 4 h into CIP treatment. The increased gene expression for several Ca^{2+} ATPase isoforms suggests that acinar cells may upregulate genes that promote a decrease in cytosolic Ca^{2+}. Analysis of the RNA-seq data for genes affecting Ca^{2+} 4 h into CIP identified expression of 193 out of a possible 254 genes (76%) linked to Ca^{2+} regulation in either saline or cerulein-treated tissue based on Gene Ontology categorization. Twenty-six genes (10.3% of all known-related Ca^{2+} genes or 13.5% of those Ca^{2+} genes expressed in the pancreas) are significantly up-regulated in that time, with an additional 21 genes (8.3% or 10.9%, respectively) down-regulated. Therefore, >24% of all genes expressed in the pancreas that affect Ca^{2+} levels are altered within 4 h of initiating CIP). Using Kyoto Encyclopedia of Genes and Genomes (KEGG) pathway, these genes were mapped to pathways affecting cytosolic Ca^{2+} (Supplementary Fig. S5). The effects of altered expression were predicted for each gene that would affect cytosolic Ca^{2+} based on the published protein function (Table 1). A distinct trend was observed in which genes encoding proteins that elevate cytosolic Ca^{2+}, such as CCKAR and IP_3R3, were significantly reduced. Conversely, several Ca^{2+} ATPase encoding genes, including *Atp2a2* and *Atp2b2*, were significantly increased. *Atp2c2c* fell within the former group suggesting that it may promote increased cytosolic Ca^{2+}.

To test this theory, HEK293 cells were transfected with GFP+/− plasmids encoding a full length myc-tagged SPCA2 ($SPCA2^{MYC}$), or a FLAG-tagged C-terminal truncated protein that completely mimicked the coding region of SPCA2C (*pcDNA3.1-SPCA2C*^{FLAG}). Examination of protein localization by co-IF analysis for $SPCA2C^{FLAG}$ and $SPCA2^{MYC}$ showed overlapping localization of the two proteins (Fig. 5). However, there were also regions of unique accumulation, indicating

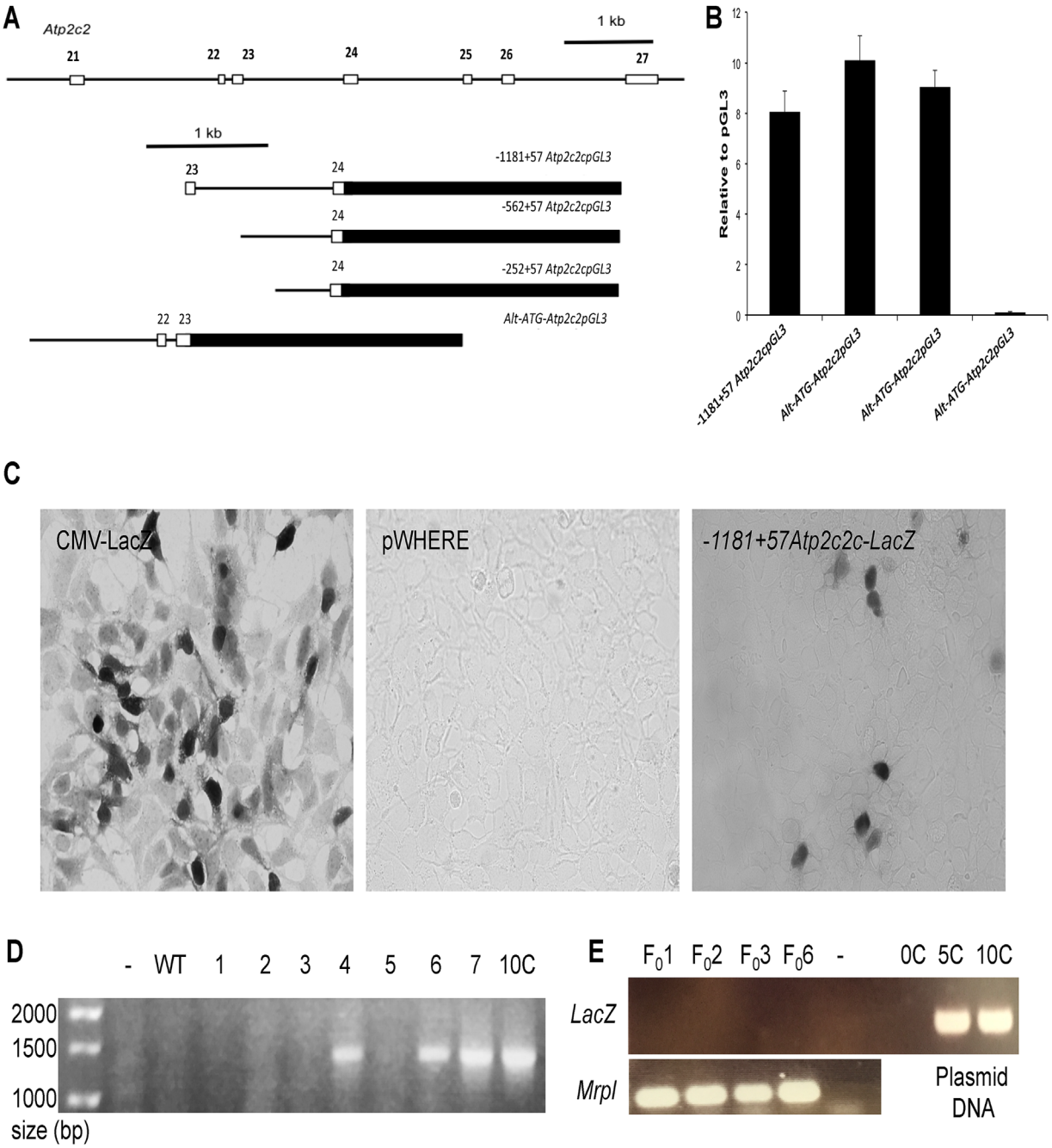

Fig. 3. The genomic region upstream of the *Atp2c2c* transcript exhibits promoter activity. A: Schematic of promoter-reporter constructs containing 1238 bp (*−1181 + 57Atp2c2cpGL3*), 619 bp (*−562 + 57Atp2c2cpGL3*), and 309 bp (*−252 + 57Atp2c2pGL3*) of sequence upstream of the *Atp2c2c* TSS. Note: these constructs contain the complete 5′ UTR for *Atp2c2c*. B: Reporter activity following transfection of luciferase reporter constructs into HEK293 $^{*}P < 0.05$. Values are normalized to luciferase activity in the *pGL3* vector that does not contain any promoter fragment. C: *LacZ* histochemistry of HEK293 cells transiently transfected with *CMV-LacZ*, *pWHERE* with no promoter, or *pWHERE* containing the *−1181 + 57Atp2c2c* region in front of *LacZ*. D: Representative PCR for transgene in genomic DNA from one litter of potential founder mice identifying three positive samples. Control is genomic DNA spiked with the equivalent of 10 copies (10C) of the transgenic plasmid. E: RT-PCR for *LacZ* RNA expression in founder mice, *Mrpl* was used as loading control and non-transgenic DNA spiked with 5 or 10 copies (C) of *1181 + 57Atp2c2cpWHERE plasmid*.

different cellular localization of the full length and SPCA2C isoforms. HEK293 cells expressing SPCA2C^{FLAG} showed a significant increase in resting cytosolic Ca^{2+} relative to GFP or SPCA2^{MYC}-expressing cells using Fura2 ratiometric analysis (Fig. 6A and B). In addition, expression of SPCA2C^{FLAG} resulted in greater increases in cytosolic Ca^{2+} following carbachol stimulation (Fig. 6A and C) while SPCA2^{MYC} showed only a trend towards significance. These results suggest that SPCA2C elevated basal cytosolic Ca^{2+} levels, opposite to the functional role of other Ca^{2+} ATPases.

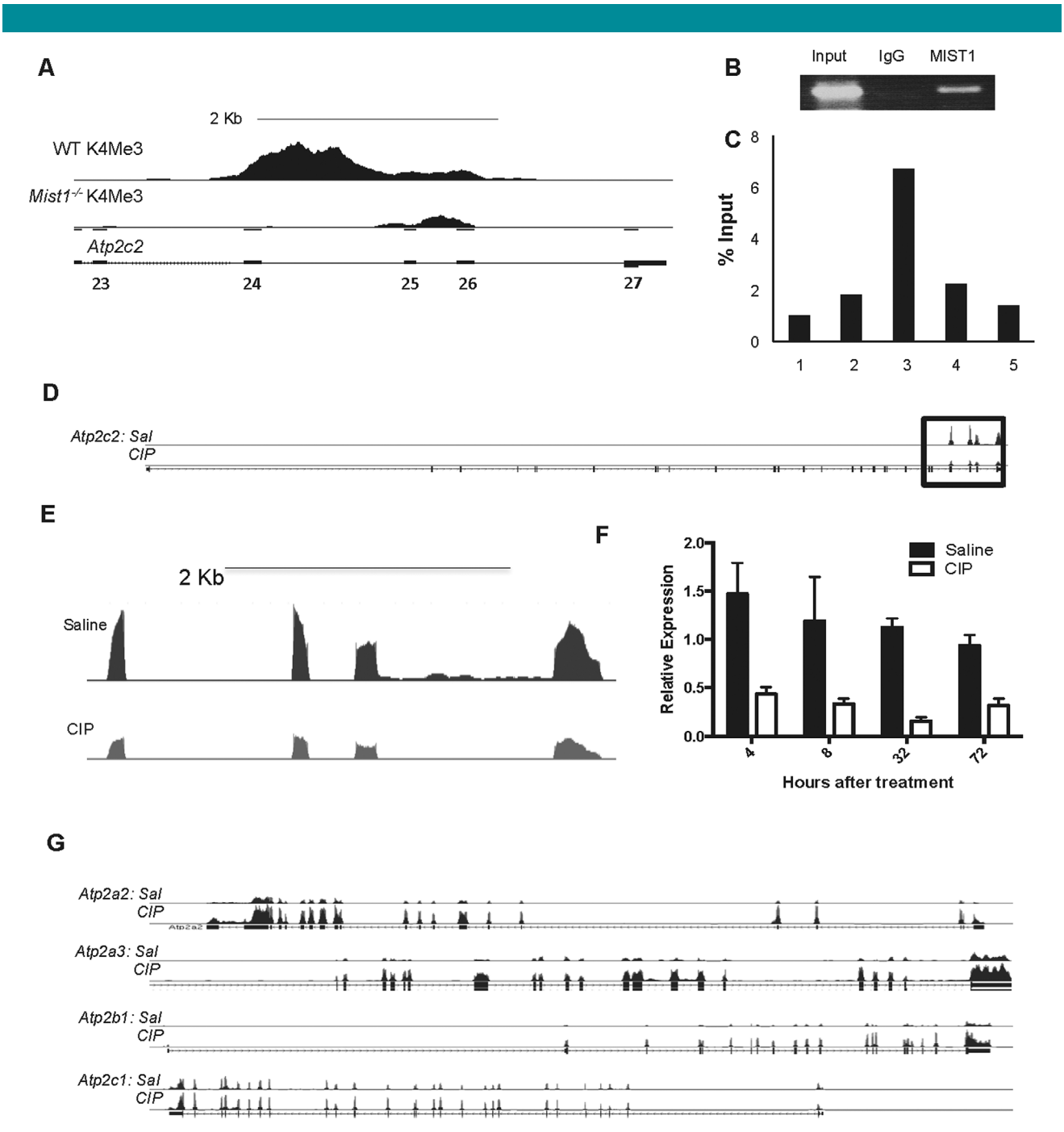

Fig. 4. ***Atp2c2c*** **expression is reduced during pancreatitis. A: Schematic showing of ChIP-seq for H3K4Me3 enrichment in WT and** ***Mist1***$^{-/-}$ **pancreatic tissue. B: ChIP-PCR and (C) ChIP-qPCR indicates MIST1 localizes to regions near exon 24 of the** ***Atp2c2*** **gene. RNA-seq at low (D) and high (E) resolution for** ***Atp2c2c*** **expression 4 h after initiating CIP. F: qRT-PCR confirms significantly reduced** ***Atp2c2c*** **expression until at least 72 h into CIP. G: Visualization of** ***Atp2*** **gene expression using the UCSC genome browser and RNA-seq tracks developed from whole pancreatic RNA obtained 4 h into cerulein or saline treatment.** ***Atp2c2c*** **expression is significantly decreased by CIP treatment, while** ***Atp2a2***, ***Atp2a3***, ***Atp2b1***, **and** ***Atp2c1*** **are all significantly reduced.**

Discussion

The importance of Ca^{2+} as a second messenger for pancreatic acinar exocytosis and cell function is well established. Ca^{2+} ATPases, including those of the PMCA and SERCA families, have key roles in acinar cell biology (Lee et al., 1997; Prasad et al., 2004). We have previously shown that SPCA2 is expressed to high levels in the pancreas (Garside et al., 2010), but little is known about its function in this tissue. In this study, we show that the novel pancreatic isoform of SPCA2 (SPCA2C) is transcribed from a novel TSS within the *Atp2c2* gene that generates a transcript that includes only the last four exons of the full length *Atp2c2* gene. The SPCA2C protein sequence aligns with the carboxy terminus of SPCA2.

TABLE 1. Expression of Ca^{2+}-regulating genes 4 hours after inducing CIP

Gene	log2 (fold change)	Effect on cytosolic Ca^{2+}	Reference[a]
Itpkc	6.25602	Remove	Li et al. (2013)
Sphk1	5.01899	—	
Ncs1	4.03756	Remove	Nakamura et al. (2011)
Cacnb2	2.68014	Add	Breitenkamp et al. (2014)
Trpc1	2.57667	Add	Willoughby et al. (2014)
Micu3	1.91612	Remove	Plovanich et al. (2013)
Atp2a2	1.69111	Remove	Ringpfeil et al. (2001)
Calm2	1.67262	—	
Atp2b1	1.38563	Remove	Strehler and Treiman (2004)
Atp2a3	1.23098	Remove	Bobe et al. (2004)
Adora2b	1.02344	—	
Calm1	0.999638	—	
Plcg2	0.956653	Add	Streb et al. (1985)
Adcy4	0.902953	—	
Adcy9	0.831247	—	
Ppp3r1	0.78638	Remove	Guerini (1997)
Plcd1	0.774936	Add	Jaken and Yuspa (1988); Punnonen et al. (1993)
Chrm3	0.750425	Add	Wess et al. (2007)
Cherp	0.709924	Add	Laplante et al. (2000)
Vdac3	0.68958	Remove	Huang et al. (2013)
Orai2	−0.660906	Add	Mercer et al. (2006)
Mcu	−0.738988	Remove	Patron et al. (2013)
P2rx1	−0.843921	Add	North (2002)
Orai3	−1.01062	Add	Mercer et al. (2006)
Itpr2	−1.08852	Add	Yamamoto-Hino et al. (1994)
Itpka	−1.09573	—	
Prkaca	−1.17005	—	
Atp2c2	−2.1948	?	
Ptger3	−1.36579	Add	Morimoto et al. (2014)
Grpr	−2.20381	Add	Xiao et al. (2003)
Gna14	−2.89861	Add	Hubbard and Hepler (2006)
Chrm1	−3.03857	Add	Wess et al. (2007)
Cckar	−4.22087	Add	Pandol et al. (1985)

[a]Effect on cytosolic Ca^{2+} was determined based on function reported in literature.

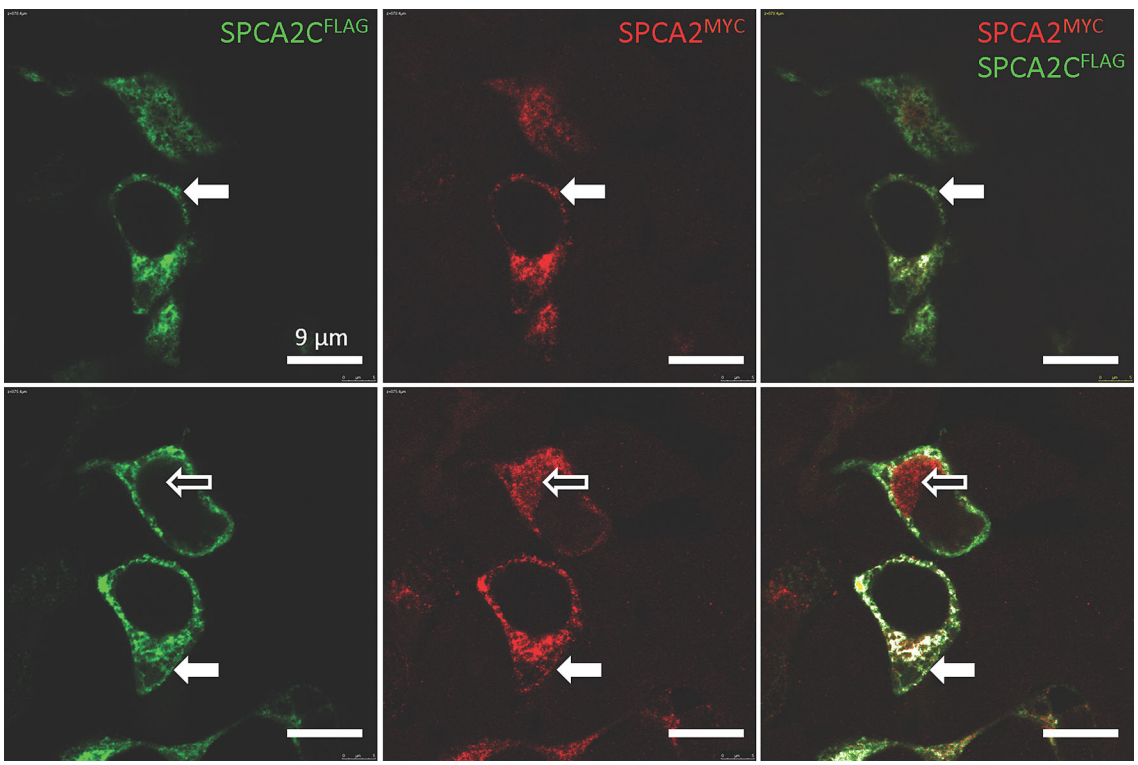

Fig. 5. Intracellular protein accumulation of SPCA2^{MYC} and SPCA2C^{FLAG}. Co-localization of *SPCA2C^{FLAG}* and *SPCA2^{MYC}* following transfection of HEK293A cells shows cellular regions that express either SPCA2C^{FLAG} (green; closed arrow) or SPCA2^{MYC} (red; open arrow), or both (white). Images represent optical Z-axis slices that are separated by 3 µm. Magnification bar is 9 µm in all parts.

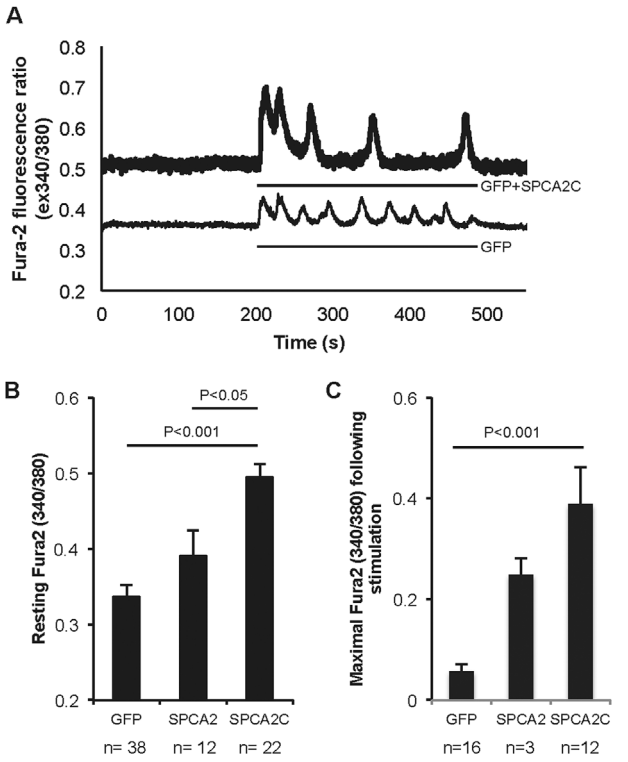

Fig. 6. SPCA2C exhibits a unique Ca^{2+} signaling function. A: Ratiometric Fura2 fluorescence analysis of single cell responses following transfection of GFP or GFP+ $SPCA2C^{FLAG}$. Lines indicate the duration of 10 μm carbachol stimulation. B: Measurement of resting cytosolic Ca^{2+} levels (before stimulation) or (C) the maximal response to carbachol stimulation show increased cytosolic Ca^{2+} levels and release only in cells transfected with $SPCA2C^{FLAG}$. *P* and N values are shown on the graphs. Cells transfected with the full length SPCA2 show a trend towards increased maximal Ca^{2+} release.

Importantly, SPCA2C shows decreased expression during CIP, and is part of a larger molecular response by the acinar cells to possibly reduce basal and stimulated cytosolic Ca^{2+} levels following acute pancreatic injury.

Most of the *Atp2* genes encode several isoforms of Ca^{2+} ATPase proteins, giving rise to extensive cell-specific expression patterns for these genes. In most cases, these isoforms are the result of alternative splicing. In the case of *Atp2c2c*, the alternative isoform expressed within the pancreas is the result of a TSS that exists within the 24th exon of the gene. Our previous reports of a pancreatic specific *Atp2c2c* transcript suggested a size of ~1.2 kb (Garside et al., 2010), significantly larger than the 702 bp transcript identified in this study. This is likely due to the different methodologies used. RNA-Seq analysis is significantly more accurate than Northern blot analysis, allowing the identification of a TSS within a few base pairs, and does not include the polyA tail that increases the size of the mature transcript. The identification of this TSS is based on high resolution RNA-seq data, combined with characterization of epigenetic modifications that are known to exist specifically at TSSs. This includes enrichment of histone marks such as H3K4Me3, H3K36Me3, and acetylated H3. Both H3K36Me3 and H3 acetylation also extend along the gene corresponding to transcription (Schwartz et al., 2009; Gunderson et al., 2011), which was observed for the *Atp2c2c* gene. At the same time, this region is enriched for RNA PolII based on targeted ChIP-PCR. Previous results indicate that *Mist1*$^{-/-}$ acini show negligible amounts of SPCA2C expression suggesting MIST1 regulates *Atp2c2c* expression (Garside et al., 2010). ChIP indicates that MIST1 directly binds in close proximity to the TSS in exon 24, and the absence of MIST1 correlates with reduced H3K4Me3, an epigenetic mark enriched at the TSS of active or primed genes (Ruthenburg et al., 2007). These results suggest that MIST1 is an important regulator of *ATP2c2c* transcription.

The 252 bp region upstream of the *Atp2c2s* TSS is sufficient to promote transcription, and the addition of an extra ~900 bp upstream of this region does not appear to increase promoter efficacy. Surprisingly, this region does not promote expression in vivo suggesting additional promoter and enhancer regions are required to recapitulate *Atp2c2* expression in the pancreas. Indeed, MIST1 enrichment appears to peak downstream of the 24th exon, and co-transfection of the *Atp2c2c* promoter reporter constructs with MIST1 did not affect promoter activity (data not shown). This suggests that the promoter regions do not include regions where MIST1 binds. While the −1181 + 57 *Atp2c2c* region tested includes several putative E boxes (binding sites for basic helix-loop-helix proteins), none of these correspond to the preferred MIST1 binding site, and analysis of the intronic region between exons 24 and 25 identified an E-box with the canonical CATATG (Tran et al., 2007) sequence preferentially targeted by MIST1 (data not shown).

Importantly, delineation of the complete transcript of *Atp2c2c* identified an open reading frame (ORF) within the transcript that encodes a 136 amino acid protein that perfectly aligns with the carboxy terminus of the full length SPCA2, hence the designation of SPCA2C. Previous work had shown that the pancreas-specific isoform contain the C terminus of the protein (Garside et al., 2010), but had not identified the exact sequence of the protein. Sequence alignment confirms that SPCA2C completely lacks four transmembrane domains, the E1–E2 hydrolase domain, a Ca^{2+} binding site, as well as other domains common to P-type ATPases suggesting that SPCA2C does not act as a Ca^{2+}ATPase in acinar cells. Nor is it likely to act as a competitor for the full length SPCA2 since both RNA-seq data and epigenetic analysis indicate non-detectable amounts of this isoform in pancreatic tissue.

In other cell types, SPCA2 affects both Ca^{2+} accumulation within the Golgi and store-independent Ca^{2+} entry (SICE; Vanoevelen et al., 2005; Faddy et al., 2008; Feng and Rao, 2013), and truncated versions of SPCA2 affect ORAI1 function in cell lines (Cross et al., 2013), suggesting a Ca^{2+} signaling role for SPCA2C. We have now confirmed that SPCA2C has both a cell localization pattern and affect on cytosolic Ca^{2+}, that is, unique from the full length SPCA2 protein. Co-localization of epitope-tagged SPCA2 and SPCA2C indicates that their localization is not identical. Since RNA-seq suggests that SPCA2C is the only isoform of *Atp2c2* expressed in the pancreas (>99% of total amount), the previous documentation of endogenous SPCA2 accumulation likely indicates only SPCA2C (Garside et al., 2010). Previous studies have shown a direct interaction of SPCA2 with ORAI channels, and the ability of C terminal regions of SPCA2 to affect SICE (Feng and Rao, 2013).

This study also suggests a global molecular response in acinar cells to reduce cytosolic Ca^{2+} levels. Genes encoding proteins that normally increase cytosolic Ca^{2+} are decreased within 4 h of inducing CIP. This includes decreases in *Atp2c2c*, which is unlike the other *Atp2* genes that either do not change expression or increase during CIP. The decreased *Atp2c2c* expression supports a function that is opposite to other Ca^{2+} ATPases and is in line with a role for SPCA2C in increasing cytosolic Ca^{2+}. As mentioned, SPCA2 interacts with ORAI1-composed plasma membrane Ca^{2+} channels, promoting SICE and Ca^{2+} influx into the cytosol (Cross et al., 2013).

Importantly, the regulation of SICE by SPCA2 is mediated through the carboxy terminus of SPCA2 (Feng and Rao, 2013). Our findings support a role in which expression of SPCA2C increases cytosolic Ca^{2+} and Ca^{2+} release following carbachol treatment. Recent studies indicate that inhibition of ORAI1 channels during pancreatitis is protective (Voronina et al., 2015), and reduced expression observed of *Atp2c2c* during CIP may be protective via decreased ORAI1 activation. Ultimately, a more complete analysis of SPCA2C function and how it affects SICE and GPCR-mediated Ca^{2+} release is needed to fully understand its role in pancreatic function. Targeted knockouts of *Atp2c2* have not been reported to date. However, this study suggests that targeting the full length *Atpc2c2* gene will not uncover a pancreatic phenotype, since using typical gene trapping strategies will leave the truncated gene and alternate TSS intact. Therefore, our identification of the novel TSS will enable more appropriate strategies for targeting *Atp2c2*.

In conclusion, this study determines that the truncated form of *Atp2c2* is transcribed from a novel TSS within the 24th exon and produces a protein that retains the C-terminus of the full-length protein. Transcription from this TSS appears to be regulated in part by MIST1 and repressed during pancreatic injury. Future studies are required to determine how SPCA2C regulates acinar cell function and how this function relates to the response of the acinar cell during pancreatic injury.

Acknowledgments

The authors wish to thank the significant contributions made to the experimental design and writing of this paper by Dr. Stephen Sims. We also would like to acknowledge Dr. Gabriel DiMattia and members of the Pin laboratory that provided helpful feedback on the study design and content of the manuscript. M.F. is supported by studentships from the Department of Pediatrics and Natural Sciences and Engineering Research Council. This work would not have been possible without the continued support of the Children's Health Foundation.

Literature Cited

Arredouani A, Guiot Y, Jonas JC, Liu LH, Nenquin M, Pertusa JA, Rahier J, Rolland JF, Shull GE, Stevens M, Wuytack F, Henquin JC, Gilon P. 2002. SERCA3 ablation does not impair insulin secretion but suggests distinct roles of different sarcoendoplasmic reticulum Ca(2+) pumps for Ca(2+) homeostasis in pancreatic beta-cells. Diabetes 51:3245–3253.

Beauvois MC, Arredouani A, Jonas JC, Rolland JF, Schuit F, Henquin JC, Gilon P. 2004. Atypical Ca2+-induced Ca2+ release from a sarco-endoplasmic reticulum Ca2+-ATPase 3-dependent Ca2+ pool in mouse pancreatic beta-cells. J. Physiol 559:141–156.

Bobe R, Bredoux R, Corvazier E, Andersen JP, Clausen JD, Dode L, Kovacs T, Enouf J. 2004. Identification, expression, function, and localization of a novel (sixth) isoform of the human sarco/endoplasmic reticulum Ca2+ ATPase 3 gene. J Biol Chem 279:24297–24306.

Breitenkamp AF, Matthes J, Nass RD, Sinzig J, Lehmkuhl G, Nurnberg P, Herzig S. 2014. Rare mutations of CACNB2 found in autism spectrum disease-affected families alter calcium channel function. PloS One 9:e95579.

Burnham DB, Williams JA. 1984. Stimulus-secretion coupling in pancreatic acinar cells. J Pediatr Gastroenterol Nutr 3Suppl 1:S1–10.

Cross BM, Hack A, Reinhardt TA, Rao R. 2013. SPCA2 regulates Orai1 trafficking and store independent Ca2+ entry in a model of lactation. PloS One 8:e67348.

Faddy HM, Smart CE, Xu R, Lee GY, Kenny PA, Feng M, Rao R, Brown MA, Bissell MJ, Roberts-Thomson SJ, Monteith GR. 2008. Localization of plasma membrane and secretory calcium pumps in the mammary gland. Biochem Biophys Res Commun 369:977–981.

Feng M, Grice DM, Faddy HM, Nguyen N, Leitch S, Wang Y, Muend S, Kenny PA, Sukumar S, Roberts-Thomson SJ, Monteith GR, Rao R. 2010. Store-independent activation of Orai1 by SPCA2 in mammary tumors. Cell 143:84–98.

Feng MY, Rao R. 2013. New insights into store-independent Ca(2+) entry: Secretory pathway calcium ATPase 2 in normal physiology and cancer. Int J Oral Sci 5:71–74.

Garside VC, Kowalik AS, Johnson CL, DiRenzo D, Konieczny SF, Pin CL. 2010. MIST1 regulates the pancreatic acinar cell expression of Atp2c2, the gene encoding secretory pathway calcium ATPase 2. Exp Cell Res 316:2859–2870.

Guerini D. 1997. Calcineurin: Not just a simple protein phosphatase. Biochem Biophys Res Commun 235:271–275.

Gunderson FQ, Merkhofer EC, Johnson TL. 2011. Dynamic histone acetylation is critical for cotranscriptional spliceosome assembly and spliceosomal rearrangements. Proc Natl Acad Sci USA 108:2004–2009.

He W, Hu Z. 2012. The role of the Golgi-resident SPCA Ca(2)(+)/Mn(2)(+) pump in ionic homeostasis and neural function. Neurochem Res 37:455–468.

Huang H, Hu X, Eno CO, Zhao G, Li C, White C. 2013. An interaction between Bcl-xL and the voltage-dependent anion channel (VDAC) promotes mitochondrial Ca2+ uptake. J Biol Chem 288:19870–19881.

Hubbard KB, Hepler JR. 2006. Cell signalling diversity of the Gqalpha family of heterotrimeric G proteins. Cell Signal 18:135–150.

Jaken S, Yuspa SH. 1988. Early signals for keratinocyte differentiation: Role of Ca2+-mediated inositol lipid metabolism in normal and neoplastic epidermal cells. Carcinogenesis 9:1033–1038.

Johnson CL, Kowalik AS, Rajakumar N, Pin CL. 2004. Mist1 is necessary for the establishment of granule organization in serous exocrine cells of the gastrointestinal tract. Mech Dev 121:261–272.

Johnson CL, Mehmood R, Laing SW, Stepniak CV, Kharitonenkov A, Pin CL. 2014. Silencing of the Fibroblast growth factor 21 gene is an underlying cause of acinar cell injury in mice lacking MIST1. Am J Physiol Endocrinol Metab 306:E916–928.

Kowalik AS, Johnson CL, Chadi SA, Weston JY, Fazio EN, Pin CL. 2007. Mice lacking the transcription factor Mist1 exhibit an altered stress response and increased sensitivity to caerulein-induced pancreatitis. Am J Physiol Gastrointest Liver Physiol 292: G1123–1132.

Kruger B, Albrecht E, Lerch MM. 2000. The role of intracellular calcium signaling in premature protease activation and the onset of pancreatitis. Am J Pathol 157:43–50.

Laplante JM, O'Rourke F, Lu X, Fein A, Olsen A, Feinstein MB. 2000. Cloning of human Ca2+ homoeostasis endoplasmic reticulum protein (CHERP): Regulated expression of antisense cDNA depletes CHERP, inhibits intracellular Ca2+ mobilization and decreases cell proliferation. Biochem J 348Pt 1:189–199.

Lee MG, Xu X, Zeng W, Diaz J, Kuo TH, Wuytack F, Racymaekers L, Muallem S. 1997. Polarized expression of Ca2+ pumps in pancreatic and salivary gland cells. Role in initiation and propagation of [Ca2+]i waves. J Biol Chem 272:15771–15776.

Li J, Zhou R, Zhang J, Li ZF. 2014. Calcium signaling of pancreatic acinar cells in the pathogenesis of pancreatitis. World J Gastroenterol 20:16146–16152.

Li P, Zhang P, Lin Y, Shan J, Wang J, Zhou T, Zhu Z, Huo K. 2013. PPP3CC feedback regulates IP3-Ca2+ pathway through preventing ITPKC degradation. Frontiers Biosci 18:919–927.

Mehmood R, Varga G, Mohanty SQ, Laing SW, Lu Y, Johnson CL, Kharitonenkov A, Pin CL. 2014. Epigenetic reprogramming in mist1(-/-) mice predicts the molecular response to cerulein-induced pancreatitis. PloS One 9:e84182.

Mercer JC, Dehaven WI, Smyth JT, Wedel B, Boyles RR, Bird GS, Putney JW Jr. 2006. Large store-operated calcium selective currents due to co-expression of Orai1 or Orai2 with the intracellular calcium sensor, Stim1. J Biol Chem 281:24979–24990.

Morimoto K, Shirata N, Taketomi Y, Tsuchiya S, Segi-Nishida E, Inazumi T, Kabashima K, Tanaka S, Murakami M, Narumiya S, Sugimoto Y. 2014. Prostaglandin E2-EP3 signaling induces inflammatory swelling by mast cell activation. J Immunol 192:1130–1137.

Nakamura TY, Jeromin A, Mikoshiba K, Wakabayashi S. 2011. Neuronal calcium sensor-1 promotes immature heart function and hypertrophy by enhancing Ca2+ signals. Circ Res 109:512–523.

North RA. 2002. Molecular physiology of P2X receptors. Physiol Rev 82:1013–1067.

Okunade GW, Miller ML, Azhar M, Andringa A, Sanford LP, Doetschman T, Prasad V, Shull GE. 2007. Loss of the Atp2c1 secretory pathway Ca(2+)-ATPase (SPCA1) in mice causes Golgi stress, apoptosis, and midgestational death in homozygous embryos and squamous cell tumors in adult heterozygotes. J Biol Chem 282:26517–26527.

Pandol SJ, Schoeffield MS, Sachs G, Muallem S. 1985. Role of free cytosolic calcium in secretagogue-stimulated amylase release from dispersed acini from guinea pig pancreas. J Biol Chem 260:10081–10086.

Patron M, Raffaello A, Granatiero V, Tosatto A, Merli G, De Stefani D, Wright L, Pallafacchina G, Terrin A, Mammucari C, Rizzuto R. 2013. The mitochondrial calcium uniporter (MCU): Molecular identity and physiological roles. J Biol Chem 288:10750–10758.

Pekowska A, Benoukraf T, Zacarias-Cabeza J, Belhocine M, Koch F, Holota H, Imbert J, Andrau JC, Ferrier P, Spicuglia S. 2011. H3K4 tri-methylation provides an epigenetic signature of active enhancers. EMBO J 30:4198–4210.

Pestov NB, Dmitriev RI, Kostina MB, Korneenko TV, Shakhparonov MI, Modyanov NN. 2012. Structural evolution and tissue-specific expression of tetrapod-specific second isoform of secretory pathway Ca2+-ATPase. Biochem Biophys Res Commun 417:1298–1303.

Pin CL, Rukstalis JM, Johnson C, Konieczny SF. 2001. The bHLH transcription factor Mist1 is required to maintain exocrine pancreas cell organization and acinar cell identity. J Cell Biol 155:519–530.

Plovanich M, Bogorad RL, Sancak Y, Kamer KJ, Strittmatter L, Li AA, Girgis HS, Kuchimanchi S, De Groot J, Speciner L, Taneja N, Oshea J, Koteliansky V, Mootha VK. 2013. MICU2, a paralog of MICU1, resides within the mitochondrial uniporter complex to regulate calcium handling. PloS One 8:e55785.

Prasad V, Okunade GW, Miller ML, Shull GE. 2004. Phenotypes of SERCA and PMCA knockout mice. Biochem Biophys Res Commun 322:1192–1203.

Punnonen K, Denning M, Lee E, Li L, Rhee SG, Yuspa SH. 1993. Keratinocyte differentiation is associated with changes in the expression and regulation of phospholipase C isoenzymes. J Invest Dermatol 101:719–726.

Ringpfeil F, Raus A, DiGiovanna JJ, Korge B, Harth W, Mazzanti C, Uitto J, Bale SJ, Richard G. 2001. Darier disease-novel mutations in ATP2A2 and genotype-phenotype correlation. Exp Dermatol 10:19–27.

Rudolph HK, Antebi A, Fink GR, Buckley CM, Dorman TE, LeVitre J, Davidow LS, Mao JI, Moir DT. 1989. The yeast secretory pathway is perturbed by mutations in PMR1, a member of a Ca2+ ATPase family. Cell 58:133–145.

Ruthenburg AJ, Allis CD, Wysocka J. 2007. Methylation of lysine 4 on histone H3: Intricacy of writing and reading a single epigenetic mark. Mol Cell 25:15–30.

Schwartz S, Meshorer E, Ast G. 2009. Chromatin organization marks exon-intron structure. Nat Struct Mol Biol 16:990–995.

Streb H, Heslop JP, Irvine RF, Schulz I, Berridge MJ. 1985. Relationship between secretagogue-induced Ca2+ release and inositol polyphosphate production in permeabilized pancreatic acinar cells. J Biol Chem 260:7309–7315.

Strehler EE, Treiman M. 2004. Calcium pumps of plasma membrane and cell interior. Curr Mol Med 4:323–335.

Sudbrak R, Brown J, Dobson-Stone C, Carter S, Ramser J, White J, Healy E, Dissanayake M, Larregue M, Perrussel M, Lehrach H, Munro CS, Strachan T, Burge S, Hovnanian A, Monaco AP. 2000. Hailey-Hailey disease is caused by mutations in ATP2C1 encoding a novel Ca(2+) pump. Hum Mol Genet 9:1131–1140.

Tran T, Jia D, Sun Y, Konieczny SF. 2007. The bHLH domain of Mist1 is sufficient to activate gene transcription. Gene Expr 13:241–253.

Vanoevelen J, Dode L, Raeymaekers L, Wuytack F, Missiaen L. 2007. Diseases involving the Golgi calcium pump. Subcell Biochem 45:385–404.

Vanoevelen J, Dode L, Van Baelen K, Fairclough RJ, Missiaen L, Raeymaekers L, Wuytack F. 2005. The secretory pathway Ca2+/Mn2+-ATPase 2 is a Golgi-localized pump with high affinity for Ca2+ ions. J Biol Chem 280:22800–22808.
Voronina S, Collier D, Chvanov M, Middlehurst B, Beckett AJ, Prior IA, Criddle DN, Begg M, Mikoshiba K, Sutton R, Tepikin AV. 2015. The role of Ca2+ influx in endocytic vacuole formation in pancreatic acinar cells. Biochem J 465:405–412.
Wess J, Eglen RM, Gautam D. 2007. Muscarinic acetylcholine receptors: Mutant mice provide new insights for drug development. Nat Rev Drug Discov 6:721–733.
Williams JA, Sans MD, Tashiro M, Schafer C, Bragado MJ, Dabrowski A. 2002. Cholecystokinin activates a variety of intracellular signal transduction mechanisms in rodent pancreatic acinar cells. Pharmacol Toxicol 91:297–303.
Willoughby D, Ong HL, De Souza LB, Wachten S, Ambudkar IS, Cooper DM. 2014. TRPC1 contributes to the Ca2+-dependent regulation of adenylate cyclases. Biochem J 464:73–84.
Xiang M, Mohamalawari D, Rao R. 2005. A novel isoform of the secretory pathway Ca2+, Mn(2+)-ATPase, hSPCA2, has unusual properties and is expressed in the brain. J Biol Chem 280:11608–11614.
Xiao D, Qu X, Weber HC. 2003. Activation of extracellular signal-regulated kinase mediates bombesin-induced mitogenic responses in prostate cancer cells. Cell Signal 15:945–953.
Yamamoto-Hino M, Sugiyama T, Hikichi K, Mattei MG, Hasegawa K, Sekine S, Sakurada K, Miyawaki A, Furuichi T, Hasegawa M, et al. 1994. Cloning and characterization of human type 2 and type 3 inositol 1,4,5-trisphosphate receptors. Recept Channels 2:9–22.
Zhao XS, Shin DM, Liu LH, Shull GE, Muallem S. 2001. Plasticity and adaptation of Ca2+ signaling and Ca2+-dependent exocytosis in SERCA2(+/−) mice. EMBO J 20:2680–2689.
Zhou W, Shen F, Miller JE, Han Q, Olson MS. 1996. Evidence for altered cellular calcium in the pathogenetic mechanism of acute pancreatitis in rats. J Surg Res 60:147–155.

Supporting Information

Additional supporting information may be found in the online version of this article at the publisher's web-site.